Spontaneous symmetry breaking without ground state degeneracy in generalized N-state clock model

Yaozong Hu and Haruki Watanabe*
Department of Applied Physics, University of Tokyo, Tokyo 113-8656, Japan

(Received 18 March 2023; revised 9 May 2023; accepted 10 May 2023; published 22 May 2023)

Spontaneous symmetry breaking is a ubiquitous phenomenon in nature. One of the defining features of symmetry-broken phases is that the large system size limit and the vanishing external field limit do not commute. In this work, we study a family of extensions of the N-state clock model. We find that the exact symmetry and the ground state degeneracy under the periodic boundary condition heavily depend on the system size, although the model has the manifest translation symmetry. In particular, the ground state can be unique and all excitations are gapped even when the phase exhibits noncommutativity of the two limits. Our model hence poses a question on the standard understanding of spontaneous symmetry breaking.

DOI: 10.1103/PhysRevB.107.195139

I. INTRODUCTION

Spontaneous breaking of symmetry is a phenomenon in which the symmetry of the Hamiltonian or the Lagrangian of the system is not respected by physical states. It underlies many phases of matter such as crystals, magnets, and superfluids, and has been studied for a long time.

To review its basic understanding, let us consider a quantum system at the zero temperature $T = 0$. For simplicity here we consider a *discrete* symmetry group, not a continuous one. Suppose that the symmetry of the system is spontaneously broken down to its subgroup. Empirically, such a phase commonly exhibits the following features: (i) The M lowest energy eigenstates in a finite system, which respect all of the original symmetries, are given as superpositions of M symmetry-breaking states. Here, M represents the number of broken symmetry elements. (ii) The splitting of the M lowest energy eigenvalues are exponentially suppressed with the system size V, while the excitation gap to the next energy level is $O(1)$. (iii) When a symmetry-breaking field ϵ that favors one of the symmetry-breaking states is introduced, the large system size limit ($V \to \infty$) and the vanishing field limit ($\epsilon \to +0$) do not commute, as illustrated in Fig. 1. The first two properties constitute the M-fold ground state degeneracy in the symmetry-broken phase that is protected by the broken symmetry of the system. The last feature implies the instability of the symmetric ground state toward an ordered state, which explains why cat states [i.e., the symmetric superpositions described in (i)] are fragile and never realized in nature. Since property (iii) is sometimes taken as the definition of spontaneous symmetry breaking [1–3], one may expect that properties (i) and (ii) follow automatically as consequences of (iii).

The transverse-field Ising model is a prototypical quantum spin model that exhibits spontaneous breaking of $\mathbb{Z}_2$ symmetry and quantum phase transition to a symmetry-unbroken phase [4]. Its generalization to an N-level spin system with $\mathbb{Z}_N$ symmetry is called the N-state clock model. The N-state clock models show all three features associated with spontaneous symmetry breaking summarized above, as we review in Sec. III A below. The quantum phase transition in the N-state clock model belongs to the same universality class as in a recent experimental study [5] of the cold atom system [6].

In this work, we introduce a generalization of the N-state clock model that shows several intriguing behaviors. This model is hinted by a recent study [7] of generalized $\mathbb{Z}_N$ toric code [8,9], whose ground state was shown to be unique for a sequence of system size despite its topological order. Our model consists of at most two-spin interactions and the nearest-neighbor interaction contains an integer parameter $a = 1, 2, \ldots, N$. The standard N-state clock model corresponds to the $a = 1$ case. When $a \neq 1$, the exact symmetry and ground state degeneracy heavily depend on the system size under the periodic boundary condition, although the model has the translation symmetry. In particular, even when a symmetry breaking occurs in the sense that the limits of large system size and vanishing symmetry-breaking field do not commute, the ground state can be unique and excitations can be gapped, depending on the system size. Hence, this model can be regarded as an example that exhibits feature (iii) without (i) and (ii).

Some previous studies of the transverse-field Ising model observed similar behaviors, but these models are different from ours in an essential way. For example, in the antiferromagnetic Ising model, the ground states are twofold degenerate and excitations are gapped for even L and excitations are gapless for odd L [10]. However, it cannot realize a unique ground state with an excitation gap. In contrast, if a symmetry-breaking external field is applied to the two spins at the ends of an open ferromagnetic Ising chain, the ground state can be unique and excitations are gapped even in the ordered phase [11]. In fact, as we will see below, our model can, in some cases, be mapped to the standard N-state clock model with a twisted boundary condition, which

*Present address: Department of Applied Physics, University of Tokyo, Tokyo 113-8656, Japan.

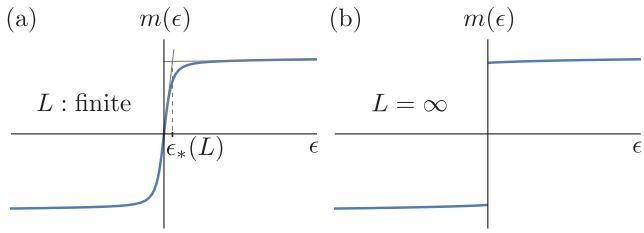

FIG. 1. Illustration of the typical behavior of an order parameter $m(\epsilon)$ as a function of symmetry-breaking field ϵ in an ordered phase. Panel (a) is for a finite L and the curve is continuous, while (b) is for the large L limit and the curve is discontinuous at $\epsilon = 0$. In panel (a), $\epsilon_*(L)$ represents the characteristic value of ϵ that separates the linear-response regime [$m(\epsilon) \propto \epsilon$] and the saturation regime. The discontinuity in (b) can be rephrased as $\lim_{L\to\infty} \epsilon_*(L) = 0$.

may be understood as an N-level version of the Ising chain with symmetry-breaking boundary condition. However, such a model lacks the translation symmetry unlike our model.

II. GENERALIZED N-STATE CLOCK MODEL

In this section, we present the definition of our generalized N-state clock model and examine its symmetries.

A. Definitions

We consider a one-dimensional system consisting of L spins. N-level ($N \geqslant 2$) spin operators are generalizations of $S = 1/2$ spin operators, satisfying

$$\hat{Z}_i \hat{X}_{i'} = \omega^{\delta_{i,i'}} \hat{X}_{i'} \hat{Z}_i, \quad \omega := e^{2\pi i/N}, \tag{1}$$

and $\hat{Z}_i^N = \hat{X}_i^N = 1$ for $i, i' = 0, 1, 2, \ldots, L-1$. The basis states $\{|\omega^\ell\rangle_i\}_{\ell=0}^{N-1}$ for the ith spin are defined by $\hat{Z}_i|\omega^\ell\rangle_i = \omega^\ell|\omega^\ell\rangle_i$ and $\hat{X}_i|\omega^\ell\rangle_i = |\omega^{\ell+1}\rangle_i$. The total Hilbert space dimension is N^L.

The Hamiltonian of our model reads as

$$\hat{H} := -\frac{1}{2}\sum_{i=0}^{L-1}\left[\left(\hat{Z}_i^{-a}\hat{Z}_{i+1} + \text{H.c.}\right) + g(\hat{X}_i + \text{H.c.})\right], \tag{2}$$

where $a = 1, 2, \ldots, N$ is an integer parameter that specifies the nearest-neighbor interaction. The standard N-state clock model corresponds to $a = 1$. The transverse field g is assumed to be non-negative. The periodic boundary condition is imposed so that $\hat{Z}_{i+L} = \hat{Z}_i$ and $\hat{X}_{i+L} = \hat{X}_i$. The energy eigenstate of $\hat{H}$ is written as $|\Phi_n\rangle$ ($n = 0, 1, 2, \ldots$) in the increasing order of the energy eigenvalues $E_0 \leqslant E_1 \leqslant E_2 \cdots$.

When $a = N$, the first term becomes the longitudinal field term $\sum_{i=1}^N(\hat{Z}_i + \text{H.c.})$ and the model is trivial. When $2 \leqslant a \leqslant N-1$, the properties of this model generally exhibit a nontrivial dependence on the system size, as we shall see below.

In our numerical study, exact diagonalization is performed up to $L = 23$ for $N = 2$, $L = 15$ for $N = 3$, and $L = 12$ for $N = 4$. Larger system sizes for $N = 3$ are handled by the density matrix renormalization group (DMRG) method using ITENSOR [12].

B. Symmetries

The symmetries of the generalized model can be divided into two classes: those which always exist, and those which might be absent depending on the system size L and the parameter a. For example, the model always has the translation symmetry $\hat{T}$, defined by

$$\hat{T}\hat{Z}_i\hat{T}^{-1} = \hat{Z}_{i+1}, \quad \hat{T}\hat{X}_i\hat{T}^{-1} = \hat{X}_{i+1}, \quad \hat{T}^L = 1. \tag{3}$$

The model also has the charge flip symmetry $\hat{C}$ [13,14] and the time-reversal symmetry $\hat{K}$ [6], defined by

$$\hat{C}\hat{Z}_i\hat{C}^{-1} = \hat{Z}_i^{-1}, \quad \hat{C}\hat{X}_i\hat{C}^{-1} = \hat{X}_i^{-1}, \quad \hat{C}^2 = 1, \tag{4}$$

$$\hat{K}\hat{Z}_i\hat{K}^{-1} = \hat{Z}_i^{-1}, \quad \hat{K}\hat{X}_i\hat{K}^{-1} = \hat{X}_i, \quad \hat{K}^2 = 1. \tag{5}$$

To be consistent with the spin algebra in Eq. (1), $\hat{C}$ is unitary and $\hat{K}$ is antiunitary. These symmetries all commute with each other.

Furthermore, depending on L and a, the model has a discrete spin-rotation symmetry generated by

$$\hat{X} := \prod_{i=0}^{L-1}\hat{X}_i^{a^i}. \tag{6}$$

We find $\hat{X}^N = 1$ and

$$\hat{X}^n\hat{H}\hat{X}^{-n} - \hat{H} = \frac{1-\omega^{n(a^L-1)}}{2}\hat{Z}_{L-1}^{-a}\hat{Z}_0 + \text{H.c.} \tag{7}$$

Therefore, if n is set to be

$$n := \frac{N}{\gcd(a^L-1, N)}, \tag{8}$$

then $n(a^L-1) = 0 \mod N$ and $[\hat{X}^n, \hat{H}] = 0$. Here, $\gcd(p, q)$ represents the greatest common divisor of integers p and q. Therefore, given N, a, and L, the exact spin-rotation symmetry of the model is given by

$$\mathbb{Z}_{\gcd(a^L-1,N)}, \tag{9}$$

implying that the ground state degeneracy in the ferromagnetically ordered phase is

$$N_{\text{deg}} = \gcd(a^L-1, N). \tag{10}$$

The operator $\hat{X}$ satisfies

$$\hat{C}\hat{X}\hat{C}^{-1} = \hat{X}^{-1}, \quad \hat{K}\hat{X}\hat{K}^{-1} = \hat{X}, \tag{11}$$

$$\hat{T}^{-1}\hat{X}\hat{T} = \hat{X}_{L-1}\prod_{i=1}^{L-1}\hat{X}_{i-1}^{a^i} = \hat{X}^a\hat{X}_{L-1}^{1-a^L}. \tag{12}$$

From the second relation, it follows that $[\hat{X}^n, \hat{T}] \neq 0$, implying that the spin-rotation symmetry $\hat{X}^n$ is not a genuine internal symmetry unless $a = 1$.

When $a = 1$, $N-1$, or N, the model also has the spatial inversion symmetry

$$\hat{I}\hat{Z}_i\hat{I}^{-1} = \hat{Z}_{-i}, \quad \hat{I}\hat{X}_i\hat{I}^{-1} = \hat{X}_{-i}, \quad \hat{I}^2 = 1. \tag{13}$$

which is explicitly broken for $a = 2, 3, \ldots, N-2$.

C. Duality

As is well known (see, e.g., Ref. [6]), the standard N-state clock model has a duality between g and $1/g$, which persists in the generalized model with $a \neq 1$ as we shall see now. Dual spin operators are defined by the nonlocal transformation

$$\hat{\tilde{Z}}_i := \prod_{i'=i}^{L-1} \hat{X}_{i'}^{a^{i'-i}} \quad (i = 0, 1, 2, \ldots, L-1) \tag{14}$$

and

$$\hat{\tilde{X}}_i := \begin{cases} \hat{Z}_{i-1}^{a} \hat{Z}_i^{-1} & (i = 1, 2, \ldots, L-1) \\ \hat{Z}_0^{-1} & (i = 0) \end{cases} \tag{15}$$

which satisfy

$$\hat{\tilde{Z}}_i^N = \hat{\tilde{X}}_i^N = 1, \quad \hat{\tilde{Z}}_i \hat{\tilde{X}}_{i'} = \omega^{\delta_{i,i'}} \hat{\tilde{X}}_{i'} \hat{\tilde{Z}}_i \tag{16}$$

for $i, i' = 0, 1, 2, \ldots, L$. This map converts $\hat{H}$ to

$$\hat{H} := -\frac{g}{2} \sum_{i=0}^{L-2} \left[\left(\hat{\tilde{Z}}_i \hat{\tilde{Z}}_{i+1}^{-a} + \text{H.c.} \right) + (1/g)(\hat{\tilde{X}}_{i+1} + \text{H.c.}) \right] - \frac{1}{2} \left[g(\hat{\tilde{Z}}_{L-1} + \text{H.c.}) + (\hat{\tilde{X}}^a \hat{\tilde{X}}_0 + \text{H.c.}) \right], \tag{17}$$

where $\hat{\tilde{X}} := \prod_{j=0}^{L-1} \hat{\tilde{X}}_j^{-a^{L-1-j}} = \hat{Z}_{L-1}$. This expression coincides with $g\hat{H}(1/g)$ except for the boundary terms and the spatial inversion. In particular, the boundary term breaks the translation invariance in terms of the dual spins even when $a = 1$. As a consequence, only the bulk properties such as the presence of an excitation gap are preserved in the duality transformation, but the order of degeneracy may be modified.

III. EXAMPLES

In this section we study the properties of the generalized models for several representative values of a.

A. $a = 1$

Let us begin by reviewing the standard N-state clock model. When $a = 1$, $\hat{X}$ in Eq. (6) has no position dependence and commutes with $\hat{H}$ regardless of L, generating a $\mathbb{Z}_N$ symmetry [i.e., $n = 1$ in Eq. (8)]. When $1 \gg g \geqslant 0$, the $\mathbb{Z}_N$ symmetry is spontaneously broken, while no symmetries are broken when $g \gg 1$. A continuous phase transition occurs at $g = 1$ for $N = 2, 3, 4$ [13,15]. There are two Berezinskii-Kosterlitz-Thouless transitions at $g = g_1$ $(1 > g_1 \geqslant 0)$ and $1/g_1$ for $N \geqslant 5$, as suggested by the aforementioned duality [13,15].

1. Order parameter, long-range order, and finite-size splitting

To diagnose spontaneous breaking of $\mathbb{Z}_N$ symmetry, let us introduce an order parameter

$$\hat{z} := \frac{1}{L} \sum_{i=0}^{L-1} \hat{Z}_i, \tag{18}$$

which transforms linearly under $\hat{X}$:

$$\hat{X}^\dagger \hat{z} \hat{X} = \omega \hat{z}. \tag{19}$$

When $g = 0$, product states

$$|\phi_\ell\rangle := \bigotimes_{i=0}^{L-1} |\omega^\ell\rangle_i = \hat{X}^\ell |\phi_0\rangle \tag{20}$$

$(\ell = 0, 1, 2, \ldots, N-1)$ are symmetry-breaking ground states, characterized by the expectation value $\langle\phi_\ell|\hat{z}|\phi_\ell\rangle = \omega^\ell$. The N-fold degeneracy is guaranteed by the $\mathbb{Z}_N$ symmetry: $[\hat{H}, \hat{X}] = 0$. In addition to the time-reversal symmetry $\hat{K}$ and the translation symmetry $\hat{T}$, the $\mathbb{Z}_2$ symmetry generated by $\hat{C}_\ell := \hat{X}^\ell \hat{C} \hat{X}^{-\ell}$ remains unbroken for each $\ell = 0, 1, 2, \ldots, N-1$. The gap to the $(N+1)$th state is given by $2(1 - \cos \frac{2\pi}{N})$.

When $g \neq 0$ but still in the range $1 \gg g > 0$, the N lowest-energy eigenstates remain separated by other excited states by an $O(1)$ excitation gap. In particular, the ground state $|\Phi_0\rangle$ in a finite system can be approximated by the linear combination $N^{-1/2} \sum_{\ell=0}^{N-1} |\phi_\ell\rangle + O(g)$. This state is symmetric, $\hat{X}|\Phi_0\rangle = |\Phi_0\rangle$, and the expectation value of the order parameter vanishes, $\langle\Phi_0|\hat{z}|\Phi_0\rangle = 0$. Instead, this state has a long-range correlation, which can be captured by the large L limit of

$$m := \sqrt{\langle\Phi_0|\hat{z}^\dagger \hat{z}|\Phi_0\rangle}. \tag{21}$$

For example, when $N = 2$, an analytic expression is known [16]:

$$\lim_{L\to\infty} m = (1 - g^2)^{1/8}. \tag{22}$$

A nonzero value of the long-range order m in the large system size limit implies spontaneous breaking of the $\mathbb{Z}_N$ symmetry [17].

The finite-size splitting of energy eigenvalues of lowest N eigenstates is typically the order of $g^L = e^{-L/\xi}$ $(\xi := -1/\ln g)$, which is exponentially suppressed with the system size. This can be most easily understood by the perturbation theory from the $g = 0$ point, since at least Lth-order perturbation is needed to generate nonzero matrix elements among $|\phi_\ell\rangle$ $(\ell = 0, 1, 2, \ldots, N-1)$. For example, when $N = 2$, the asymptotic behavior for a large L is given by [18]

$$\Delta_1 := E_1 - E_0 \simeq 2\sqrt{\frac{1 - g^2}{\pi L}} g^L [1 + O(L^{-1})]. \tag{23}$$

For reader's convenience, we include the derivation of Eqs. (22) and (23) in the Appendix. By exact diagonalization, we confirm the validity of these analytic expressions by numerics in Figs. 2(a)–2(c). For $N \geqslant 3$, such expressions are not known but we numerically demonstrate that the $N = 3$ case behaves similarly in Figs. 2(d)–2(f).

2. Symmetry-breaking field

Another way to detect spontaneous symmetry breaking is to apply a symmetry-breaking field $\epsilon \geqslant 0$ [3]. We replace the Hamiltonian $\hat{H}$ with

$$\hat{H}^{(\ell_0)}(\epsilon) := \hat{H} - \tfrac{1}{2}\epsilon L(\omega^{-\ell_0}\hat{z} + \text{H.c.}). \tag{24}$$

The parameter $\ell_0 = 0, 1, \ldots, N-1$ selects the symmetry-breaking state favored by $\epsilon > 0$. As far as the $\mathbb{Z}_N$ symmetry

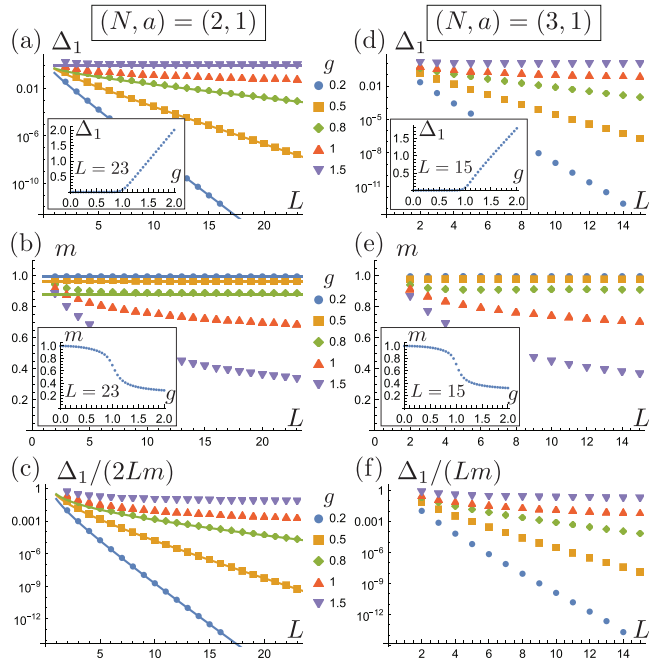

FIG. 2. Exact-diagonalization results for the standard N-state clock model with $N = 2$ (a)–(c) and $N = 3$ (d)–(f). (a),(d) The energy difference $\Delta_1 := E_1 - E_0$ between the ground state and the first excited state in a finite system, which decays exponentially with L in the ordered phase ($1 > g \geqslant 0$) and stays constant in the disordered phase ($g > 1$). (b),(e) The long-range order $m := \sqrt{\langle\Phi_0|\hat{z}^\dagger\hat{z}|\Phi_0\rangle}$, which converges to a nonzero value in the ordered phase ($1 > g \geqslant 0$) and decays with L in the disordered phase ($g > 1$). (c),(f) $\Delta_1/(2Lm)$ (c) and $\Delta_1/(Lm)$ (f) that approximate $\epsilon_*(L)$. The insets in (a), (b), (d), and (e) show the g dependence. The curves in (a)–(c) are the analytic expressions in Eqs. (22), (23), and (27).

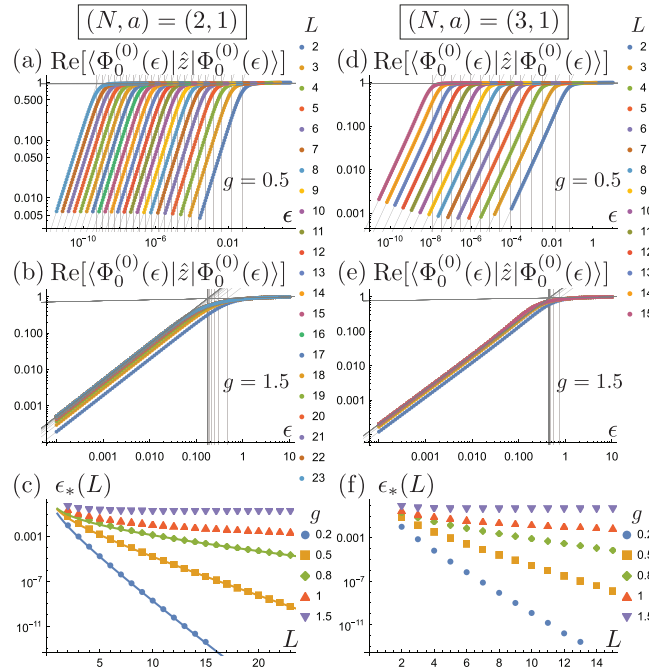

FIG. 3. Exact-diagonalization results for the standard N-state clock model with symmetry-breaking field ϵ for $N = 2$ (a)–(c) and for $N = 3$ (d)–(f). Here we set $\ell_0 = 0$ as an example. (a),(b),(d),(e) The order parameter $\mathrm{Re}[\langle\Phi_0^{(0)}(\epsilon)|\hat{z}|\Phi_0^{(0)}(\epsilon)\rangle]$ for $g = 0.5$ (a),(c) and $g = 1.5$ (b),(e). (c),(f) The magnetic field $\epsilon_*(L)$ at the transition point, which is determined by the crossing point of two fitting lines (gray lines) in the log-log plot of $\mathrm{Re}[\langle\Phi_0^{(0)}(\epsilon)|\hat{z}|\Phi_0^{(0)}(\epsilon)\rangle]$. The curves in (c) are the analytic expression in Eq. (27).

generated by $\hat{X}$ is exact, all values of ℓ_0 are equivalent in the sense that they are related by the $\mathbb{Z}_N$ symmetry.

The effect of symmetry-breaking field can be understood analytically based on the effective Hamiltonian that focuses on the N low-energy states. For example, for $N = 2, 3, 4$, we find

$$H_{\mathrm{eff}}^{(\ell_0)}(\epsilon) = -\frac{c_N\Delta_1}{2}(X + \mathrm{H.c.}) - \frac{\epsilon Lm}{2}(\omega^{-\ell_0}Z + \mathrm{H.c.}) \quad (25)$$

in the basis of symmetry-breaking states, where $c_2 = 1/2$, $c_3 = 2/3$, and $c_4 = 1$, and

$$X := \begin{pmatrix} & & 1 \\ 1 & & \\ & \ddots & \\ & 1 & \end{pmatrix}, \quad Z := \begin{pmatrix} 1 & & & \\ & \omega & & \\ & & \ddots & \\ & & & \omega^{N-1} \end{pmatrix}. \quad (26)$$

The first term describes the mixing due to $g \neq 0$, and the second term favors the symmetry-breaking state that matches the applied field.

For a small ϵ, the order parameter $\mathrm{Re}[\langle\omega^{-\ell_0}Z\rangle]$ exhibits the linear response $\mathrm{Re}[\langle\omega^{-\ell_0}Z\rangle] \propto Lm^2\epsilon/\Delta_1$, while it is saturated $\mathrm{Re}[\langle\omega^{-\ell_0}Z\rangle] \simeq m$ for a large ϵ. The transition occurs at $\epsilon = \epsilon_*(L)$ where the first term and second term balance. We find

$$\epsilon_*^{N=2}(L) \simeq \frac{\Delta_1}{2Lm} \simeq \frac{(1-g^2)^{3/8}}{\sqrt{\pi}L^{3/2}}g^L, \quad (27)$$

$$\epsilon_*^{N=3,4}(L) \simeq \frac{\Delta_1}{Lm}. \quad (28)$$

It follows that

$$\lim_{L\to\infty} \epsilon_*(L) = 0, \quad (29)$$

implying the discontinuity in the expectation value of the order parameter as a function of ϵ in the thermodynamic limit. This observation suggests that the small ϵ limit and the large L limit do not commute:

$$\lim_{\epsilon\to+0}\lim_{L\to\infty} \left\langle\Phi_0^{(\ell_0)}(\epsilon)\middle|\hat{z}\middle|\Phi_0^{(\ell_0)}(\epsilon)\right\rangle \neq 0, \quad (30)$$

$$\lim_{L\to\infty}\lim_{\epsilon\to+0} \left\langle\Phi_0^{(\ell_0)}(\epsilon)\middle|\hat{z}\middle|\Phi_0^{(\ell_0)}(\epsilon)\right\rangle = 0, \quad (31)$$

where $|\Phi_0^{(\ell_0)}(\epsilon)\rangle$ is the unique ground state of $\hat{H}^{(\ell_0)}(\epsilon)$.

We confirm this understanding by numerical calculations in Fig. 3. Panels (a) and (c) for $N = 2$ and panels (b) and (d) for $N = 3$ demonstrate that the expectation value of the order parameter develops as the symmetry-breaking field ϵ increases, and saturates around $\epsilon = \epsilon_*(L)$. The system size dependence is qualitatively different between the ordered phase [Figs. 3(a) and 3(d)] and the disordered phase [Figs. 3(b) and 3(e)]. As shown in Figs. 3(c) and 3(f), the saturation field

$\epsilon_*(L)$ gets smaller and smaller as the system size increases and vanishes in the large L limit in the ordered phase, while it converges to a nonzero value in the disordered phase. As explained in the caption of Fig. 1, this is the numerical demonstration of the noncommutative nature of the two limits in Eqs. (30) and (31) in the symmetry-breaking phase of the $a = 1$ model.

B. N is odd and $a = N - 1$

Next, let us study the simplest nontrivial case. When $a = N - 1$, the Hamiltonian becomes

$$\hat{H} := -\frac{1}{2}\sum_{i=0}^{L-1}\left[(\hat{Z}_i\hat{Z}_{i+1} + \text{H.c.}) + g(\hat{X}_i + \text{H.c.})\right], \tag{32}$$

which is still manifestly translation invariant.

1. L: Even

Let us first assume that L is even. In this case, the model has a modified $\mathbb{Z}_N$ symmetry generated by

$$\hat{X} := \prod_{i=0}^{L-1}\hat{X}_i^{(-1)^i} = \hat{X}_0\hat{X}_1^\dagger\hat{X}_2\hat{X}_3^\dagger\cdots\hat{X}_{L-2}\hat{X}_{L-1}^\dagger. \tag{33}$$

In other words, n in Eq. (8) is 1. The corresponding order parameter

$$\begin{aligned}\hat{z} &:= \frac{1}{L}\sum_{i=0}^{L-1}\hat{Z}_i^{(-1)^i} \\ &= \frac{1}{L}(\hat{Z}_0 + \hat{Z}_1^\dagger + \hat{Z}_2 + \hat{Z}_3^\dagger + \cdots + \hat{Z}_{L-2} + \hat{Z}_{L-1}^\dagger)\end{aligned} \tag{34}$$

satisfies Eq. (19). This model can be mapped to the standard one with $a = +1$ by the $\hat{C}$ transformation in Eq. (4) for spins only on even sites. Therefore, as far as thermodynamic properties are concerned, the $a = N - 1$ model should be equivalent to the standard $a = +1$ model. In particular, when $N = 3$, the $\mathbb{Z}_N$ symmetry of the model is spontaneously broken when $1 > g \geqslant 0$ and a phase transition to the paramagnetic phase occurs at $g = 1$.

When $g = 0$, the ferromagnetic state $|\phi_0\rangle := \bigotimes_{i=0}^{L-1}|1\rangle_i$ is a ground state. N distinct ground states can be generated as

$$|\phi_\ell\rangle := \hat{X}^\ell|\phi_0\rangle = \bigotimes_{i=0}^{L-1}|\omega^{\ell(-1)^i}\rangle_i, \tag{35}$$

whose expectation value of order parameter is $\langle\phi_\ell|\hat{z}|\phi_\ell\rangle = \omega^\ell$ ($\ell = 0, 1, 2, \ldots, N-1$). Interestingly, $|\phi_\ell\rangle$ with $\ell \neq 0$ is not translation invariant, i.e., $\hat{T}|\phi_\ell\rangle = |\phi_{-\ell}\rangle$. It is instead symmetric under a modified translation symmetry $\hat{T}_\ell := \hat{T}\hat{X}^{-2\ell}$.

2. L: Odd

Next let us assume that L is odd. In this case,

$$\hat{X} := \prod_{i=0}^{L-1}\hat{X}_i^{(-1)^i} = \hat{X}_0\hat{X}_1^\dagger\hat{X}_2\hat{X}_3^\dagger\cdots\hat{X}_{L-2}^\dagger\hat{X}_{L-1} \tag{36}$$

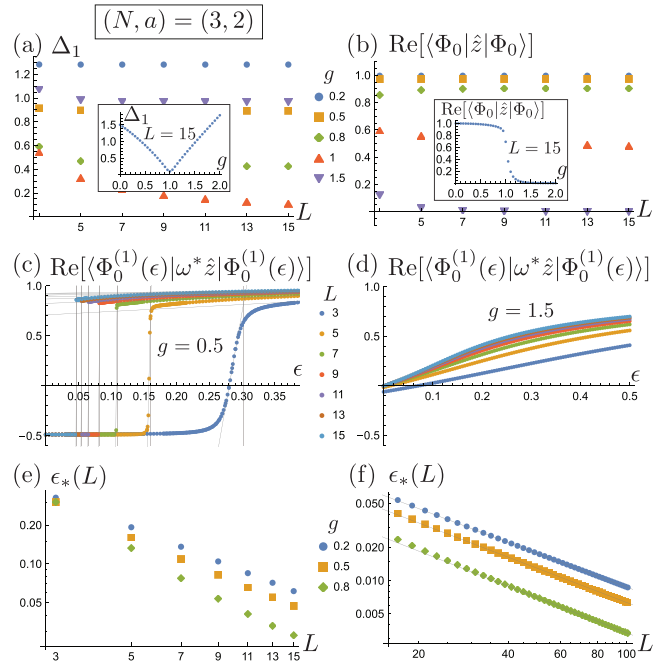

FIG. 4. Exact diagonalization results (a)–(e) and DMRG results (f) for the $(N, a) = (3, 2)$ case. (a) The energy difference $\Delta_1 = E_1 - E_0$. (b) The order parameter $\text{Re}[\langle\Phi_0|\hat{z}|\Phi_0\rangle]$. The insets in (a) and (b) show the g dependence. (c),(d) $\text{Re}[\langle\Phi_0^{(1)}(\epsilon)|\omega^*\hat{z}|\Phi_0^{(1)}(\epsilon)\rangle]$ for $g = 0.5$ (c) and $g = 1.5$ (d). (e) The magnetic field $\epsilon_*(L)$ at the transition point, which is determined by the crossing points of two fitting lines in panel (c). (f) The same as (e) but for larger system size ($17 \leqslant L \leqslant 101$) computed by DMRG. The fitting lines have slope -1 with few percent error, confirming the L^{-1} dependence of $\epsilon_*(L)$.

does not commute with $\hat{H}$ in Eq. (32):

$$\hat{X}^\dagger\hat{H}\hat{X} - \hat{H} = \frac{1-\omega^2}{2}\hat{Z}_{L-1}\hat{Z}_0 + \text{H.c.} \tag{37}$$

Furthermore, n in Eq. (8) is N and $\hat{X}^n$ becomes the identity operator. As a consequence, the ground state is unique and excitations are gapped even in the range $1 > g \geqslant 0$. We show our numerical results for $N = 3$ in Fig. 4(a).

Unlike the even L case, the unique ground state has a nonzero expectation value of the order parameter $\text{Re}[\langle\Phi_0|\hat{z}|\Phi_0\rangle]$ when $0 \leqslant g < 1$ as shown in Fig. 4(b), where

$$\begin{aligned}\hat{z} &:= \frac{1}{L}\sum_{i=0}^{L-1}\hat{Z}_i^{(-1)^i} \\ &= \frac{1}{L}(\hat{Z}_0 + \hat{Z}_1^\dagger + \hat{Z}_2 + \hat{Z}_3^\dagger + \cdots + \hat{Z}_{L-2}^\dagger + \hat{Z}_{L-1}).\end{aligned} \tag{38}$$

This nonzero expectation value is allowed by the absence of an exact spin-rotation symmetry.

Despite the lack of symmetry, we observe that the energy difference $\Delta_1 := E_1 - E_0$ between the ground state and the first excited state vanishes at $g = 1$, implying the presence of a quantum phase transition of two phases at this point. See the inset of Fig. 4(a). This is expected from our results for the even L case, where a transition from the ordered phase ($1 > g \geqslant 0$) to the disordered phase ($g > 1$) occurs at $g = 1$. The thermodynamic behaviors, such as the presence or absence of

a phase transition, must be insensitive to the detailed choice of the system size.

Indeed, even in this case, one can still form the Hamiltonian $\hat{H}^{(\ell_0=1)}(\epsilon)$ in Eq. (24) with a symmetry-breaking field, where $\hat{H}$ is given by Eq. (32) and $\hat{z}$ is given by Eq. (38). In Figs. 4(c) and 4(d), we show our numerical results on the expectation value $\mathrm{Re}[\langle\Phi_0^{(\ell_0=1)}(\epsilon)|\omega^*\hat{z}|\Phi_0^{(\ell_0=1)}(\epsilon)\rangle]$. The results for $1 > g \geqslant 0$ [Fig. 4(c)] and $g > 1$ [Fig. 4(d)] clearly show qualitatively different behaviors. In particular, when $1 > g \geqslant 0$, we observe that $\mathrm{Re}[\langle\Phi_0^{(1)}(\epsilon)|\omega^*\hat{z}|\Phi_0^{(1)}(\epsilon)\rangle]$ is negative for $0 \leqslant \epsilon \ll \epsilon_*(L)$ and jumps to a positive value at $\epsilon = \epsilon_*(L)$. As shown in Figs. 4(e) and 4(f), the transition field $\epsilon_*(L)$ vanishes in the large L limit, implying that the large L limit and the vanishing ϵ limit do not commute:

$$0 < \lim_{\epsilon\to+0}\lim_{L\to\infty}\left\langle\Phi_0^{(\ell_0)}(\epsilon)\middle|\hat{z}\middle|\Phi_0^{(\ell_0)}(\epsilon)\right\rangle \neq \lim_{L\to\infty}\lim_{\epsilon\to+0}\left\langle\Phi_0^{(\ell_0)}(\epsilon)\middle|\hat{z}\middle|\Phi_0^{(\ell_0)}(\epsilon)\right\rangle < 0. \tag{39}$$

Note that both $\lim_{\epsilon\to+0}\lim_{L\to\infty}\langle\Phi_0^{(\ell_0)}(\epsilon)|\hat{z}|\Phi_0^{(\ell_0)}(\epsilon)\rangle$ and $\lim_{L\to\infty}\lim_{\epsilon\to+0}\langle\Phi_0^{(\ell_0)}(\epsilon)|\hat{z}|\Phi_0^{(\ell_0)}(\epsilon)\rangle$ are nonzero in this case, unlike Eq. (31).

The scaling of $\epsilon_*(L)$ is qualitatively different depending on the parity of L. As we saw in Sec. III A 2, $\epsilon_*(L)$ decays exponentially with the system size in the standard model ($a = 1$) and in the $a = N - 1$ model with even L, while it only decays algebraically when the system size is odd for the $a = N - 1$ case as shown in Figs. 4(e) and 4(f) for $N = 3$. This behavior of $\epsilon_*(L)$ can also be explained by focusing on low-energy states. Here we consider only two states, $|\Phi_0\rangle$ and $\hat{X}^{\ell_0}|\Phi_0\rangle$. At $\epsilon = 0$, the energy expectation value of the latter state is greater than the former one by an amount $\Delta \sim O(1)$. However, the latter state is favored by the symmetry-breaking field. This suggests that the transition occurs at

$$\epsilon_*(L) \simeq \frac{\Delta}{\left[1-\cos\left(\frac{2\pi\ell_0}{N}\right)\right]Lm} \propto \frac{1}{L} \quad (\ell_0 \neq 0). \tag{40}$$

This is consistent with Fig. 4(f).

3. Avoiding gap closing

When the system size L is odd in the $a = N - 1$ case, no exact symmetry of the model in Eq. (32) prohibits us from adding the longitudinal magnetic field term

$$\hat{H}(\epsilon_0) = \hat{H} - \frac{\epsilon_0}{2}\sum_{i=0}^{L-1}(\hat{Z}_i + \hat{Z}_i^\dagger). \tag{41}$$

When $\epsilon_0 \neq 0$, the unique ground state for $g = 0$ and $g = 2$ can be smoothly connected without a gap closing, as demonstrated numerically by Fig. 5 for $N = 3$.

This observation suggests that the gap closing and the phase transition in odd system size were protected by the symmetry for the even system size. Namely, reference to the even L system was mandatory for the discussion of odd L system.

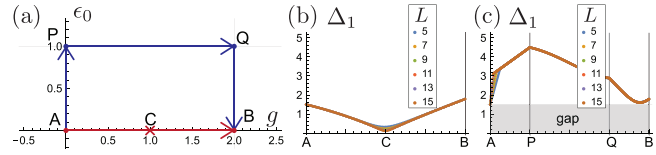

FIG. 5. Exact-diagonalization results for the $(N, a) = (3, 2)$ case. (a) Paths in the (g, ϵ_0) plane. When A: (0,0) is directly connected to B: (2,0) (red arrow), a quantum phase transition occurs at C: (1,0). However, when bypassed via P: (0,1) and Q: (1,1) (blue arrows), the transition can be avoided. (b),(c) $\Delta_1 = E_1 - E_0$ for the red path (b) and the blue path (c) in panel (a). To check the convergence as a function of the system size, the results for $L = 5, 7, \ldots, 15$ are shown.

C. $a = 0 \mod \mathrm{rad}(N)$

As the last example, let us discuss the case in which the ground state for $g = 0$ and $g = \infty$ can be adiabatically connected to each other without a gap closing, implying the uniqueness of the phase and the absence of any sort of phase transitions.

When N is factorized as $N = \prod_j p_j^{r_j}$, the radical of N is defined as $\mathrm{rad}(N) := \prod_j p_j$. For example, $\mathrm{rad}(N) = 2$ for $N = 4 = 2^2$. When a is a multiple of $\mathrm{rad}(N)$, the $\mathbb{Z}_N$ symmetry is absent [i.e., n in Eq. (8) is N] regardless of the system size L. As a consequence, the ground state is unique and excitations are gapped regardless of g.

The simplest example of this situation is when $N = 4$ and $a = 2$. We show our numerical results in Fig. 6. Clearly, the gap remains open as g is changed from 0 to 2 for any value of L.

IV. CONCLUSION

In this work, we introduced a generalized N-state clock model which contains an integer parameter $a = 1, 2, \ldots, N$ [Eq. (2)]. The original N-state clock model corresponds to the $a = 1$ case. When $a \neq 1$, the spin-rotation symmetry [Eq. (7)] and the ground state degeneracy in the ordered phase under the periodic boundary condition [Eq. (10)] strongly depend on the system size L.

In particular, when a is $N - 1$ and both N and L are odd, the spin-rotation symmetry is absent [Eq. (37)] and the ground state is unique even in the ordered phase [Fig. 4(a)], despite the fact that a spontaneous "symmetry" breaking is suggested by the noncommutativity of the large system size limit and the vanishing external field limit [Eq. (39)]. In contrast, when L is even, the same model has the $\mathbb{Z}_N$ symmetry and exhibits

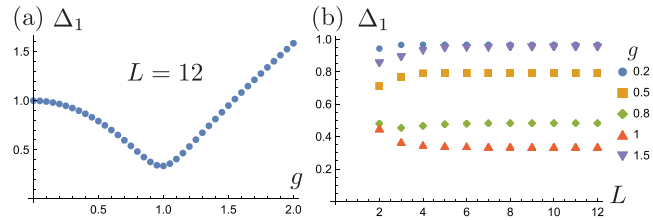

FIG. 6. Exact-diagonalization results for the $(N, a) = (4, 2)$ case. $\Delta_1 = E_1 - E_0$ as a function of (a) g and (b) L.

spontaneous symmetry breaking in the standard manner (see Sec. III B 1). Since thermodynamic properties should be insensitive to the details of the systems size or the boundary condition, this model with odd L should be counted as an example of spontaneous symmetry breaking without exact symmetry or degeneracy. Indeed, we numerically found a gap closing at $g = 1$.

The $a = N - 1$ model can be mapped to the standard N-state clock model ($a = +1$) by the $\hat{C}$ transformation in Eq. (4) for spins on even sites. When L is odd, this transformation introduces a defect for the spins at $i = L$ and $i = 1$, which may be viewed as a boundary condition $\hat{Z}_L^\dagger = \hat{Z}_0$. This defect breaks the translation symmetry and the $\mathbb{Z}_N$ symmetry, explaining the absence of the ground state degeneracy. However, other values of a cannot be mapped to the $a = 1$ model and the degeneracy pattern cannot be understood in this way.

Although our model itself might be difficult to be realized in experiments, the importance of our example lies in the fact that it exemplifies the coexistence of a spontaneous symmetry breaking and a unique ground state with a finite excitation gap in a translationally invariant spin model with short-ranged interactions. The excitation gap closes at the transition point to the disordered phase. Knowing this possibility is particularly important when one investigates interacting spin models numerically—one often concludes the absence of any spontaneous symmetry breaking based on the uniqueness of the ground state, but our example draws caution in such a reasoning.

ACKNOWLEDGMENTS

We thank Y. Fuji, S. Ono, H. Kobayashi, Z. Xiong, and H. Katsura for useful discussions. The work of H.W. is supported by JSPS KAKENHI Grants No. JP20H01825 and No. JP21H01789.

APPENDIX: EXACT SOLUTION FOR $N = 2$

We review the exact solution of the transverse-field Ising model via the Jordan-Wigner transformation following Refs. [16,18–21].

1. Jordan-Wigner transformation

$N = 2$ level spins can be represented by fermion operators:

$$\hat{X}_i = (\hat{f}_i + \hat{f}_i^\dagger)\prod_{i'=0}^{i-1}(-1)^{\hat{f}_{i'}^\dagger \hat{f}_{i'}}, \tag{A1}$$

$$\hat{Z}_i = (-1)^{\hat{f}_i^\dagger \hat{f}_i} = 1 - 2\hat{f}_i^\dagger \hat{f}_i = \hat{f}_i \hat{f}_i^\dagger - \hat{f}_i^\dagger \hat{f}_i, \tag{A2}$$

where $\prod_{i'=0}^{i-1}(-1)^{\hat{f}_{i'}^\dagger \hat{f}_{i'}} = 1$ when $i = 0$. The product state $|\Phi_0\rangle = \bigotimes_{i=0}^{L-1}|1\rangle_i$ is mapped to the Fock vacuum $|0\rangle$. The definition of the Jordan-Wigner transformation here is slightly different from the standard one [16,19–21] but we find that this choice is more useful in that expressions in Eqs. (A9) and (A11) below do not depend on the parity of L.

Interchanging the role of $\hat{X}_i$ and $\hat{Z}_i$, we find

$$\begin{aligned}\hat{H} &= -\sum_{i=0}^{L-1}\hat{X}_{i+1}\hat{X}_i - g\sum_{i=0}^{L-1}\hat{Z}_i \\ &= -\sum_{i=0}^{L-2}(\hat{f}_{i+1}^\dagger + \hat{f}_{i+1})(\hat{f}_i - \hat{f}_i^\dagger) \\ &\quad - [-(-1)^{\hat{N}}](\hat{f}_0^\dagger + \hat{f}_0)(\hat{f}_{L-1} - \hat{f}_{L-1}^\dagger) \\ &\quad - g\sum_{i=0}^{L-1}(1 - 2\hat{f}_i^\dagger \hat{f}_i).\end{aligned} \tag{A3}$$

In the $(-1)^{\hat{N}} = +1$ (-1) sector, we set the boundary condition to be antiperiodic $\hat{f}_{L+i} = -\hat{f}_i$ (periodic $\hat{f}_{L+i} = \hat{f}_i$). With this understanding, the Hamiltonian can be rewritten as

$$\begin{aligned}\hat{H} &= -\sum_{i=0}^{L-1}(\hat{f}_{i+1}^\dagger \hat{f}_i + \hat{f}_i^\dagger \hat{f}_{i+1} + \hat{f}_{i+1}\hat{f}_i + \hat{f}_i^\dagger \hat{f}_{i+1}^\dagger) \\ &\quad + g\sum_{i=0}^{L-1}(\hat{f}_i^\dagger \hat{f}_i - \hat{f}_i \hat{f}_i^\dagger).\end{aligned} \tag{A4}$$

Introducing the Fourier transformation $\hat{f}_j^\dagger = L^{-1/2}\sum_k \hat{f}_k^\dagger e^{-ikj}$, where $k \in K_{\mathrm{AP}} = \{(2j+1)\pi/L\}_{j=0}^{L-1}$ for the antiperiodic case and $k \in K_{\mathrm{P}} = \{(2j)\pi/L\}_{j=0}^{L-1}$ for the periodic case, we find

$$\begin{aligned}\hat{H} &= \sum_k (\hat{f}_k^\dagger \quad \hat{f}_{-k})\begin{pmatrix} g - \cos k & -i\sin k \\ i\sin k & -g + \cos k \end{pmatrix}\begin{pmatrix} \hat{f}_k \\ \hat{f}_{-k}^\dagger \end{pmatrix} \\ &= \sum_k \varepsilon(k)(\hat{f}_k^\dagger \quad \hat{f}_{-k})(\cos 2\phi_k \sigma_3 + \sin 2\phi_k \sigma_2)\begin{pmatrix} \hat{f}_k \\ \hat{f}_{-k}^\dagger \end{pmatrix} \\ &= \sum_k \varepsilon(k)(\hat{\gamma}_k^\dagger \quad \hat{\gamma}_{-k})\sigma_3\begin{pmatrix} \hat{\gamma}_k \\ \hat{\gamma}_{-k}^\dagger \end{pmatrix} \\ &= \sum_k 2\varepsilon_k \hat{\gamma}_k^\dagger \hat{\gamma}_k - \sum_k \varepsilon_k.\end{aligned} \tag{A5}$$

In the derivation, we defined

$$\varepsilon(k) = \sqrt{(g - \cos k)^2 + \sin^2 k} = \sqrt{1 + g^2 - 2g\cos k}, \tag{A6}$$

$$\cos 2\phi_k = \frac{g - \cos k}{\varepsilon_k}, \quad \sin 2\phi_k = \frac{\sin k}{\varepsilon_k}, \tag{A7}$$

$$\begin{pmatrix} \hat{\gamma}_k \\ \hat{\gamma}_{-k}^\dagger \end{pmatrix} = e^{-i\phi_k \sigma_1}\begin{pmatrix} \hat{f}_k \\ \hat{f}_{-k}^\dagger \end{pmatrix} = \begin{pmatrix} \cos\phi_k & -i\sin\phi_k \\ -i\sin\phi_k & \cos\phi_k \end{pmatrix}\begin{pmatrix} \hat{f}_k \\ \hat{f}_{-k}^\dagger \end{pmatrix}. \tag{A8}$$

The last expression of Eq. (A5) implies that the ground states are those annihilated by $\hat{\gamma}_k$ for all k.

For $k = \pi$, $g - \cos k = g + 1 > 0$ regardless of $g \geqslant 0$. Hence, $\phi_{k=\pi} = 0$ and $\hat{\gamma}_{k=\pi} = \hat{f}_{k=\pi}$. On the other hand, for $k = 0$, $g - \cos k = g - 1 > 0$ and $\phi_{k=0} = 0$ and $\hat{\gamma}_{k=0} = \hat{f}_{k=0}$ only when $g > 1$. In contrast, when $1 > g \geqslant 0$, $\phi_{k=0} = \pi/2$ and $\hat{\gamma}_{k=0} = \hat{f}_{k=0}^\dagger$.

2. Ground state energy

The state

$$|\Phi_0\rangle = \prod_{k\in K_{\rm AP}} (\cos\phi_k + i\sin\phi_k \hat{f}_k^\dagger \hat{f}_{-k}^\dagger)|0\rangle \tag{A9}$$

satisfies $\hat{\gamma}_k|\Phi_0\rangle = 0$ for any $k \in K_{\rm AP}$ and hence is the ground state in the even fermion parity sector. The energy eigenvalue is given by

$$E_0(g) = -\sum_{k\in K_{\rm AP}} \varepsilon_k = -\sum_{j=0}^{L-1} \varepsilon\left(\tfrac{(2j+1)\pi}{L}\right). \tag{A10}$$

This result is valid for any $g \geqslant 0$.

On the other hand, the state

$$|\Phi_1\rangle = \hat{f}_{k=0}^\dagger \prod_{k\in K_{\rm P}, k\neq 0} (\cos\phi_k + i\sin\phi_k \hat{f}_k^\dagger \hat{f}_{-k}^\dagger)|0\rangle \tag{A11}$$

is the ground state in the odd fermion parity sector. It satisfies $\hat{\gamma}_k|\Phi_1\rangle = 0$ for any $k \in K_{\rm P}$ when $1 > g \geqslant 0$. When $1 > g$, $\gamma_{k=0}|\Phi_1\rangle$ does not vanish but this state remains the ground state in this sector because ε_k is the monotonically increasing function of $|k|$ in the range $0 \leqslant |k| \leqslant \pi$. The energy eigenvalue is given by

$$E_1(g) = -\sum_{k\in K_{\rm P}} \varepsilon_k = -\sum_{j=0}^{L-1} \varepsilon\left(\tfrac{2\pi j}{L}\right). \tag{A12}$$

When $1 > g$, $2(g-1)$ should be added to $E_1(g)$.

Comparing $E_0(g)$ and $E_1(g)$, we find $E_1(g) > E_0(g)$ whenever $g > 0$. Thus $|\Phi_0\rangle$ is the ground state in the finite system and $|\Phi_1\rangle$ is the quasidegenerate first excited state in a finite system. To evaluate the difference $E_1(g) - E_0(g)$ for $1 > g \geqslant 0$, we follow the prescription given in Ref. [22]. We first perform Fourier transformation:

$$\varepsilon_n = \int_0^{2\pi} \frac{dk}{2\pi} \varepsilon(k) e^{-ink} = \int_0^{2\pi} \frac{dk}{2\pi} \varepsilon(k)\cos nk, \tag{A13}$$

$$\varepsilon(k) = \sum_{n=-\infty}^{\infty} \varepsilon_n e^{ink} = \varepsilon_0 + 2\sum_{n=1}^{\infty} \varepsilon_n \cos nk. \tag{A14}$$

In terms of these Fourier components, $E_0(g)$ and $E_1(g)$ can be expressed as

$$E_0(g) = -\sum_{n=-\infty}^{\infty} \varepsilon_n e^{i(n\pi/L)} \sum_{j=0}^{L-1} e^{i(2n\pi/L)j} = -L\sum_{n=-\infty}^{\infty} \varepsilon_{mL}(-1)^m$$

$$= -L\varepsilon_0 - 2L\sum_{m=1}^{\infty} \varepsilon_{mL}(-1)^m \tag{A15}$$

and

$$E_1(g) = -\sum_{n=-\infty}^{\infty} \varepsilon_n \sum_{j=0}^{L-1} e^{i(2\pi n/L)j} = -L\sum_{m=-\infty}^{\infty} \varepsilon_{mL}$$

$$= -L\varepsilon_0 - 2L\sum_{m=1}^{\infty} \varepsilon_{mL}. \tag{A16}$$

Therefore, we get

$$E_1(g) - E_0(g) = -4L\sum_{m=0}^{\infty} \varepsilon_{(1+2m)L}$$

$$= -4L\sum_{m=0}^{\infty} \int_0^{2\pi} \frac{dk}{2\pi} \varepsilon(k) e^{i(1+2m)Lk}. \tag{A17}$$

To examine the asymptotic behavior of this integral, we introduce $\lambda > 0$ by $\lambda = -\ln g$ ($e^{-\lambda} = g$) so that

$$e^{i(k+i\lambda)} = e^{ik}g, \quad e^{-i(k+i\lambda)} = e^{-ik}/g. \tag{A18}$$

It follows that

$$\varepsilon(k+i\lambda) = \sqrt{(e^{ik}-1)(e^{-ik}-g^2)}, \tag{A19}$$

$$e^{i(1+2m)L(k+i\lambda)} = e^{i(1+2m)Lk} g^{(1+2m)L}. \tag{A20}$$

Since $\varepsilon(z)e^{i(1+2m)Lz}$ is analytic when $|{\rm Im}z| \leqslant \lambda$, the integration path can be shifted from the real axis to $k+i\lambda$ with $k \in [0, 2\pi]$. We find

$$E_1(g) - E_0(g) = 4L\sum_{m=0}^{\infty} g^{(1+2m)L} I_{(1+2m)L}(g), \tag{A21}$$

where

$$I_L(g) := -\int_0^{2\pi} \frac{dk}{2\pi} \sqrt{(e^{ik}-1)(e^{-ik}-g^2)}\, e^{iLk}$$

$$= \frac{\Gamma\left(L-\frac{1}{2}\right)}{\sqrt{4\pi}\,\Gamma(L+1)} {}_2F_1\left(-\frac{1}{2}, L-\frac{1}{2}; L+1; g^2\right) \tag{A22}$$

and ${}_2F_1(a,b;c;z)$ is the hypergeometric function. The sum over m in Eq. (A21) is clearly dominated by the $m = 0$ contribution. Therefore, we obtain the asymptotic form for $L \to \infty$:

$$E_1(g) - E_0(g)$$

$$\simeq \frac{2L\,\Gamma\left(L-\frac{1}{2}\right) g^L}{\sqrt{\pi}\,\Gamma(L+1)} {}_2F_1\left(-\frac{1}{2}, L-\frac{1}{2}; L+1; g^2\right) + O(g^{3L})$$

$$\simeq \left(1 + \frac{3(1+g^2)}{8(1-g^2)L} + \frac{5(5g^4-22g^2+5)}{128(1-g^2)^2L^2}\right.$$

$$\left. + \frac{105(1+g^2)^3}{1024(1-g^2)^3L^3} + O(L^{-4})\right) 2\sqrt{\frac{1-g^2}{\pi L}}\, g^L. \tag{A23}$$

The leading term was previously derived in Ref. [18]. The $O(L^{-m})$ ($m = 1, 2, 3$) corrections were not found in literature, and higher-order corrections can be computed in the same way.

3. Long-range correlation

Next, let us investigate the correlation functions.

$$\hat{X}_i\hat{X}_{i+n} = (\hat{f}_i + \hat{f}_i^\dagger) \prod_{j=i}^{i+n-1} (-1)^{\hat{f}_j^\dagger \hat{f}_j} (\hat{f}_{i+n} + \hat{f}_{i+n}^\dagger)$$

$$= (\hat{f}_i^\dagger - \hat{f}_i) \prod_{j=i+1}^{i+n-1} (\hat{f}_j^\dagger + \hat{f}_j)(\hat{f}_j^\dagger - \hat{f}_j)(\hat{f}_{i+n}^\dagger + \hat{f}_{i+n})$$

$$= \hat{B}_i\hat{A}_{i+1}\hat{B}_{i+1}\hat{A}_{i+2}\cdots\hat{B}_{i+n-1}\hat{A}_{i+n}, \tag{A24}$$

where $\hat{A}_i \coloneqq \hat{f}_i^\dagger + \hat{f}_i$ and $\hat{B}_i \coloneqq \hat{f}_i^\dagger - \hat{f}_i$, which satisfy $\{\hat{A}_i, \hat{B}_j\} = 0$ and $\{\hat{A}_i, \hat{A}_j\} = -\{\hat{B}_i, \hat{B}_j\} = 2\delta_{ij}$.

We are interested in the correlation function with respect to the ground state $|\Phi_0\rangle$. According to Wick's theorem, the correlation function can be decomposed into the sum of two point functions:

$$\langle \hat{X}_i \hat{X}_{i+n} \rangle = \langle \hat{B}_i \hat{A}_{i+1} \hat{B}_{i+1} \hat{A}_{i+2} \cdots \hat{B}_{i+n-1} \hat{A}_{i+n} \rangle = \sum_\sigma \mathrm{sgn}(\sigma) \prod_{j=i}^{i+n-1} \langle \hat{B}_j \hat{A}_{\sigma(j)+1} \rangle. \tag{A25}$$

Using

$$\hat{f}_i = \frac{1}{\sqrt{L}} \sum_{k \in K_{\mathrm{AP}}} e^{iki} (\cos\phi_k \hat{\gamma}_k + i \sin\phi_k \hat{\gamma}_{-k}^\dagger) \tag{A26}$$

and $\hat{\gamma}_k |\Phi_0\rangle = 0$, we get

$$\langle \hat{f}_i^\dagger \hat{f}_j^\dagger \rangle = -\langle \hat{f}_i \hat{f}_j \rangle = \frac{i}{2L} \sum_{k \in K_{\mathrm{AP}}} e^{ik(i-j)} \frac{\sin k}{\varepsilon_k}, \tag{A27}$$

$$\langle \hat{f}_i \hat{f}_j^\dagger \rangle = \langle \hat{f}_j \hat{f}_i^\dagger \rangle = \frac{1}{2L} \sum_{k \in K_{\mathrm{AP}}} e^{ik(i-j)} \left(1 + \frac{g - \cos k}{\varepsilon_k} \right), \tag{A28}$$

$$\langle \hat{f}_i^\dagger \hat{f}_j \rangle = \langle \hat{f}_j^\dagger \hat{f}_i \rangle = \frac{1}{2L} \sum_{k \in K_{\mathrm{AP}}} e^{ik(i-j)} \left(1 - \frac{g - \cos k}{\varepsilon_k} \right), \tag{A29}$$

from which we find

$$\langle \hat{A}_i \hat{A}_j \rangle = \langle \hat{f}_i^\dagger \hat{f}_j^\dagger + \hat{f}_i \hat{f}_j + \hat{f}_i^\dagger \hat{f}_j + \hat{f}_i \hat{f}_j^\dagger \rangle = \delta_{ij}, \tag{A30}$$

$$\langle \hat{B}_i \hat{B}_j \rangle = \langle \hat{f}_i^\dagger \hat{f}_j^\dagger + \hat{f}_i \hat{f}_j - \hat{f}_i^\dagger \hat{f}_j - \hat{f}_i \hat{f}_j^\dagger \rangle = -\delta_{ij}, \tag{A31}$$

$$\langle \hat{B}_i \hat{A}_j \rangle = \langle \hat{f}_i^\dagger \hat{f}_j^\dagger - \hat{f}_i \hat{f}_j + \hat{f}_i^\dagger \hat{f}_j - \hat{f}_i \hat{f}_j^\dagger \rangle = G_{j-i-1}. \tag{A32}$$

Here we defined

$$G_m \coloneqq \langle \hat{B}_i \hat{A}_{m+i+1} \rangle = \frac{1}{L} \sum_{k \in K_{\mathrm{AP}}} \frac{1 - g e^{ik}}{\varepsilon_k} e^{ikm} = \frac{1}{L} \sum_{k \in K_{\mathrm{AP}}} \sqrt{\frac{1 - g e^{ik}}{1 - g e^{-ik}}} e^{ikm} \simeq \int_0^{2\pi} \frac{dk}{2\pi} G(e^{-ik}) e^{ikm} \tag{A33}$$

and

$$G(e^{-ik}) = \sqrt{\frac{1 - g e^{ik}}{1 - g e^{-ik}}}. \tag{A34}$$

Therefore, the correlation function in Eq. (A25) can be written as the determinant of a Toeplitz matrix:

$$\langle \hat{X}_i \hat{X}_{i+n} \rangle \simeq \begin{vmatrix} G_0 & G_{-1} & G_{-2} & \cdots & G_{1-n} \\ G_1 & G_0 & G_{-1} & \cdots & G_{2-n} \\ G_2 & G_1 & G_0 & \cdots & G_{3-n} \\ \vdots & \vdots & \vdots & & \vdots \\ G_{n-1} & G_{n-2} & G_{n-3} & \cdots & G_0 \end{vmatrix}, \tag{A35}$$

whose asymptotic behavior is given by the strong Szegö limit theorem [20,21].

$$\langle \hat{X}_i \hat{X}_{i+n} \rangle \simeq (e^{d_0})^n e^{\sum_{n=1}^\infty n d_n d_{-n}} = (1 - g^2)^{1/4}, \tag{A36}$$

where

$$d_0 = \int_0^{2\pi} \frac{dk}{2\pi} \ln[G(e^{-ik})] = 0, \tag{A37}$$

$$d_n = \int_0^{2\pi} \frac{dk}{2\pi} \ln[G(e^{-ik})] e^{ikn} = \frac{g^{|n|}}{2n}. \tag{A38}$$

This result implies [16]

$$\lim_{L \to \infty} m(g) = (1 - g^2)^{1/8}. \tag{A39}$$

[1] A. Auerbach, *Interacting Electrons and Quantum Magnetism* (Springer, New York, 1998).

[2] A. Altland and B. D. Simons, *Condensed Matter Field Theory*, 2nd ed. (Cambridge University Press, Cambridge, UK, 2010).

[3] H. Tasaki, *Physics and Mathematics of Quantum Many-Body Systems* (Springer, New York, 2020).

[4] S. Sachdev, *Quantum Phase Transitions*, 2nd ed. (Cambridge University Press, Cambridge, UK, 2011).

[5] H. Bernien, S. Schwartz, A. Keesling, H. Levine, A. Omran, H. Pichler, S. Choi, A. S. Zibrov, M. Endres, M. Greiner, V. Vuletić, and M. D. Lukin, Nature (London) **551**, 579 (2017).

[6] S. Whitsitt, R. Samajdar, and S. Sachdev, Phys. Rev. B **98**, 205118 (2018).

[7] H. Watanabe, M. Cheng, and Y. Fuji, J. Math. Phys. **64**, 051901 (2023).

[8] E. Dennis, A. Kitaev, A. Landahl, and J. Preskill, J. Math. Phys. **43**, 4452 (2002).

[9] A. Kitaev, Ann. Phys. **303**, 2 (2003).

[10] J.-J. Dong, P. Li, and Q.-H. Chen, J. Stat. Mech.: Theory Exp. (2016) 113102.

[11] A. Pelissetto, D. Rossini, and E. Vicari, Phys. Rev. E **98**, 032124 (2018).

[12] M. Fishman, S. R. White, and E. M. Stoudenmire, SciPost Phys. Codebases 4 (2022).

[13] G. Ortiz, E. Cobanera, and Z. Nussinov, Nucl. Phys. B **854**, 780 (2012).

[14] N. Moran, D. Pellegrino, J. K. Slingerland, and G. Kells, Phys. Rev. B **95**, 235127 (2017).

[15] G. Sun, T. Vekua, E. Cobanera, and G. Ortiz, Phys. Rev. B **100**, 094428 (2019).

[16] P. Pfeuty, Ann. Phys. **57**, 79 (1970).

[17] T. A. Kaplan, P. Horsch, and W. von der Linden, J. Phys. Soc. Jpn. **58**, 3894 (1989).

[18] G. G. Cabrera and R. Jullien, Phys. Rev. B **35**, 7062 (1987).

[19] E. Lieb, T. Schultz, and D. Mattis, Ann. Phys. **16**, 407 (1961).

[20] B. M. McCoy, *Advanced Statistical Mechanics* (Oxford University Press, New York, 2009).

[21] S. Suzuki, J.-i. Inoue, and B. K. Chakrabarti, *Quantum Ising Phases and Transitions in Transverse Ising Models* (Springer, New York, 2012), Vol. 862.

[22] M. N. Barber and M. E. Fisher, Ann. Phys. **77**, 1 (1973).